Electronic Supporting Information (ESI) for Dalton Transactions.
This journal is © The Royal Society of Chemistry 2020

Mirror-image magnetic circularly polarized luminescence (MCPL) from optically inactive Eu^{III} and Tb^{III} tris(β-diketonate)

Hiroki Yoshikawa,[a] Gaku Nakajima,[a] Yuki Mimura,[a] Takahiro Kimoto,[a] Yoshiro Kondo,[b] Satoko Suzuki,[b] Michiya Fujiki[c]* and Yoshitane Imai[a]*

a Department of Applied Chemistry, Faculty of Science and Engineering, Kindai University, 3-4-1 Kowakae, Higashi-Osaka, Osaka 577-8502, Japan.
b JASCO Corporation, 2967-5 Ishikawa-machi Hachioji-shi Tokyo Japan 192-8537, Japan.
c Graduate School of Materials Science, Nara Institute of Science and Technology, 8916-5 Takayama, Ikoma, Nara 630-0192, Japan.

*Corresponding author. Tel.: (YI) +81 06 6730 5880x5241; fax: (YI) +81 06 6727 2024; e-mail: (YI) y-imai@apch.kindai.ac.jp, (MF) fujikim@ms.naist.jp.

Table of Contents

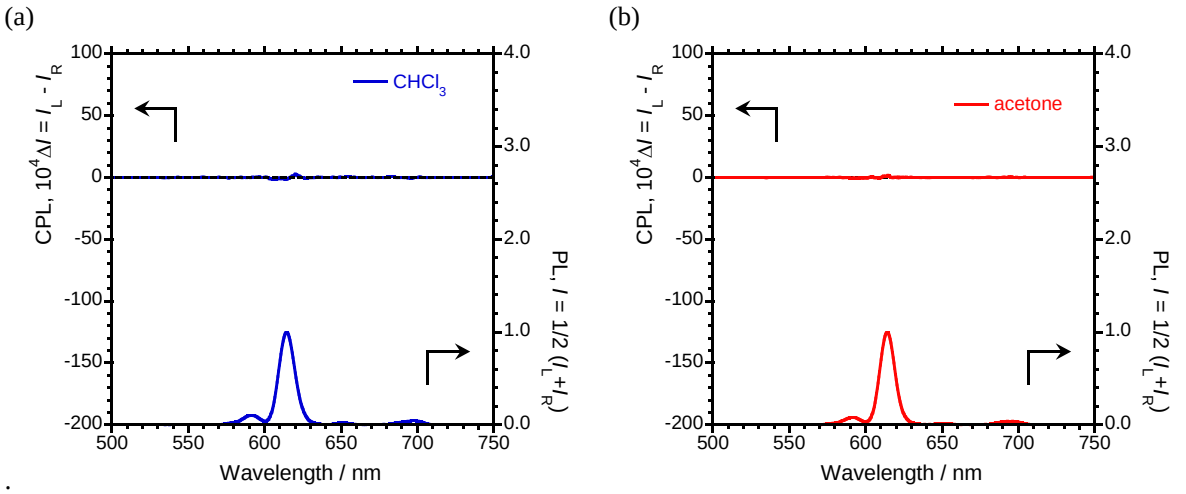

Fig. S1. Comparison of CPL (upper panel) and PL (lower panel) spectra of $Eu^{III}(hfa)_3$ in (a) $CHCl_3$ and (b) acetone for 1.0×10^{-3} M, ($CHCl_3$: λ_{ex} = 300 nm. and acetone : λ_{ex} = 330 nm. Path length = 5 mm.

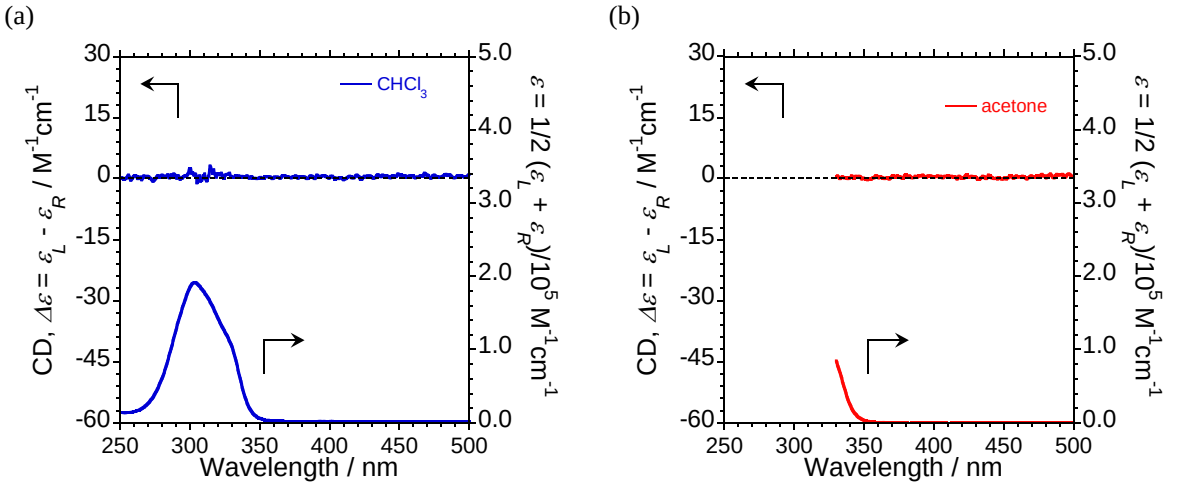

Fig. S2. Comparison of CD (upper panel) and UV (lower panel) spectra of $Eu^{III}(hfa)_3$ in (a) $CHCl_3$ and (b) acetone for 1.0×10^{-3} M, ($CHCl_3$: λ_{ex} = 300 nm. and acetone : λ_{ex} = 330 nm. Path length = 1 mm.

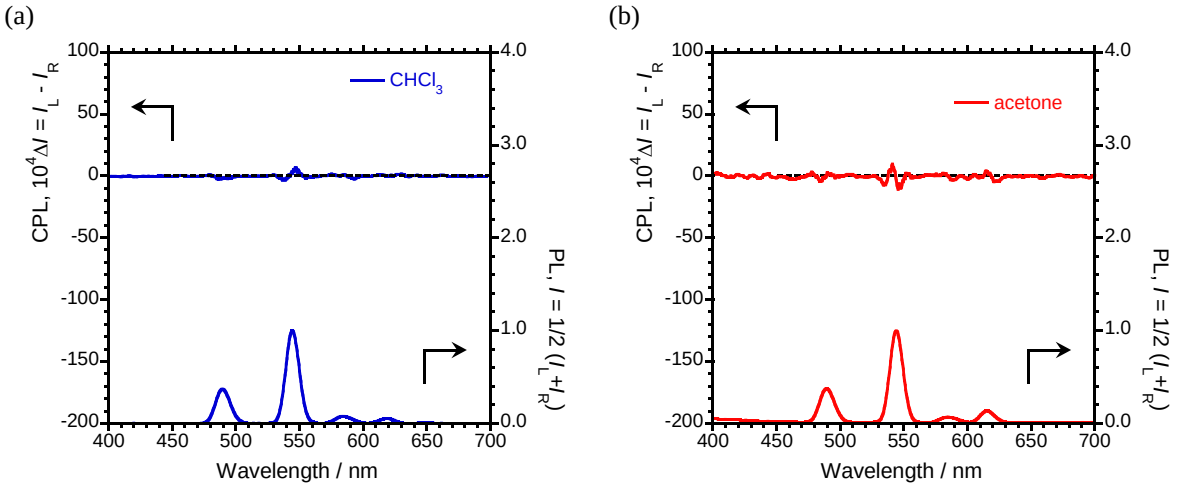

Fig. S3. Comparison of CPL (upper panel) and PL (lower panel) spectra of $Tb^{III}(hfa)_3$ in (a) $CHCl_3$ and (b) acetone for 1.0×10^{-3} M, ($CHCl_3$: λ_{ex} = 300 nm. and acetone : λ_{ex} = 330 nm. Path length = 5 mm.

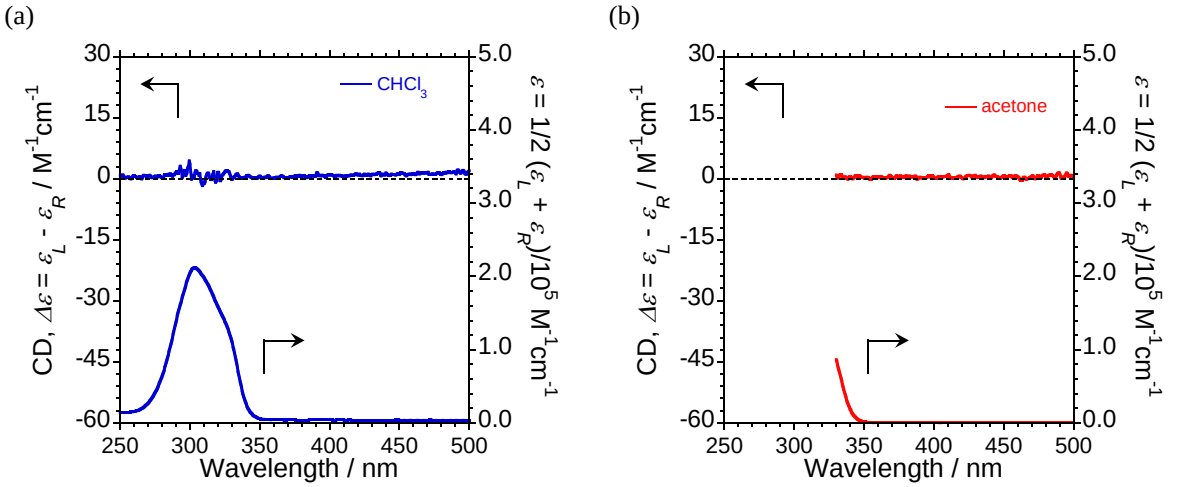

Fig. S4. Comparison of CD (upper panel) and UV (lower panel) spectra of $Tb^{III}(hfa)_3$ in (a) $CHCl_3$ and (b) acetone for 1.0×10^{-3} M, ($CHCl_3$: λ_{ex} = 300 nm. and acetone : λ_{ex} = 330 nm. Path length = 1 mm.

Table S1. MCPL properties of $Eu^{III}(hfa)_3$ in PMMA film, KBr pellet and powder states under 1.6 T.

Entry	State	λ_{MCPL} (nm)	$\lvert g_{MCPL}\rvert$ ($10^{-2}T^{-1}$)	λ_{MCPL} (nm)	$\lvert g_{MCPL}\rvert$ ($10^{-2}T^{-1}$)	λ_{MCPL} (nm)	$\lvert g_{MCPL}\rvert$ ($10^{-2}T^{-1}$)	λ_{MCPL} (nm)	$\lvert g_{MCPL}\rvert$ ($10^{-2}T^{-1}$)
1	PMMA-film	587	0.75	598	0.81	610	0.63	620	0.58
		689	1.7	703	1.5				
2	KBr-pellet	587	0.69	596	0.63	609	0.58	619	0.51
		689	1.4	704	1.2				
3	Powder	587	0.18	596	0.11	609	0.094	620	0.046
		688	0.22	705	0.22				

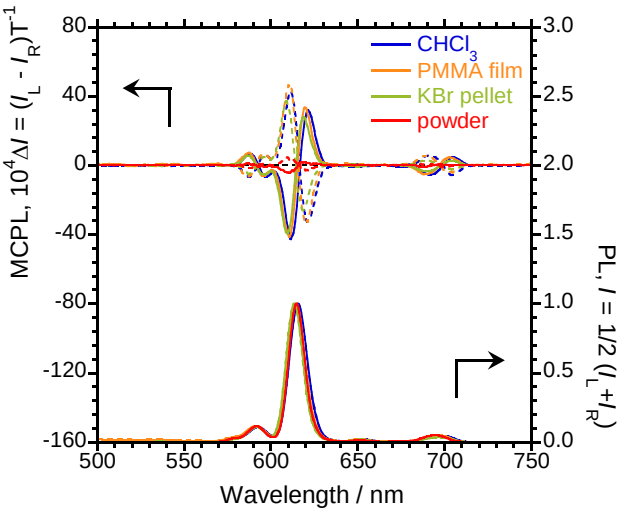

Fig. S5. MCPL (upper panel) and PL (lower panel) spectra of $Eu^{III}(hfa)_3$ in N-up (solid lines) and S-up (dotted lines) configurations under 1.6 T in $CHCl_3$ (blue lines) (1.0×10^{-3} m) in PMMA film (orange lines), KBr pellet (green lines) and powder (red lines) states.

Table S2. MCPL properties of $Tb^{III}(hfa)_3$ in PMMA film, KBr pellet and powder states under 1.6 T.

Entry	State	λ_{MCPL} (nm)	$\lvert g_{MCPL}\rvert$ ($10^{-2}T^{-1}$)	λ_{MCPL} (nm)	$\lvert g_{MCPL}\rvert$ ($10^{-2}T^{-1}$)	λ_{MCPL} (nm)	$\lvert g_{MCPL}\rvert$ ($10^{-2}T^{-1}$)	λ_{MCPL} (nm)	$\lvert g_{MCPL}\rvert$ ($10^{-2}T^{-1}$)
1	PMMA-film	483	0.39	495	0.54	540	0.061	555	0.26
		579	0.41	589	0.88	616	0.47	626	0.88
2	KBr-pellet	483	0.28	493	0.21	539	0.068	553	0.068
		578	0.43	588	0.58	616	0.075	626	0.59
3	Powder	482	0.14	494	0.081	539	0.0081	553	0.036
		577	0.20	589	0.20	615	0.075	626	0.19

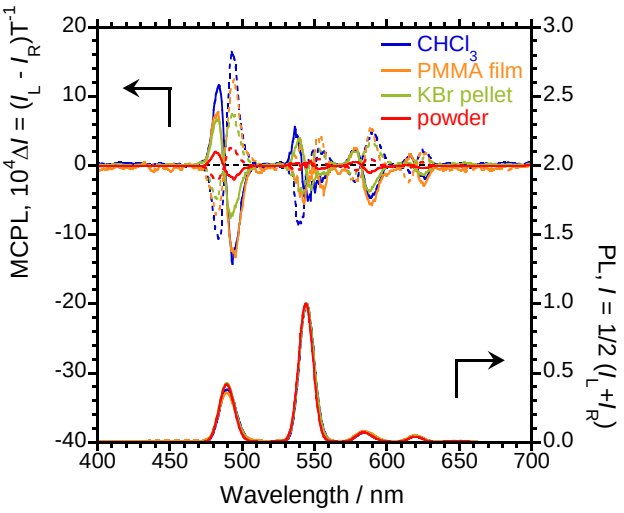

Fig. S6. MCPL (upper panel) and PL (lower panel) spectra of $Tb^{III}(hfa)_3$ in N-up (solid lines) and S-up (dotted lines) configurations under 1.6 T in $CHCl_3$ (blue lines) (1.0×10^{-3} m) in PMMA film (orange lines), KBr pellet (green lines) and powder (red lines) state.

Table S3. MCPL properties of $Tb^{III}(acac)_3$•Phen in $CHCl_3$ (1.0×10^{-3} M) under 1.6 T.

Entry	State	λ_{MCPL} (nm)	$\lvert g_{MCPL}\rvert$ ($10^{-2}T^{-1}$)	λ_{MCPL} (nm)	$\lvert g_{MCPL}\rvert$ ($10^{-2}T^{-1}$)	λ_{MCPL} (nm)	$\lvert g_{MCPL}\rvert$ ($10^{-2}T^{-1}$)	λ_{MCPL} (nm)	$\lvert g_{MCPL}\rvert$ ($10^{-2}T^{-1}$)
1	$CHCl_3$	482	0.69	494	0.49	539	0.23	549	0.094
		578	0.75	592	1.1	613	0.36	627	0.81

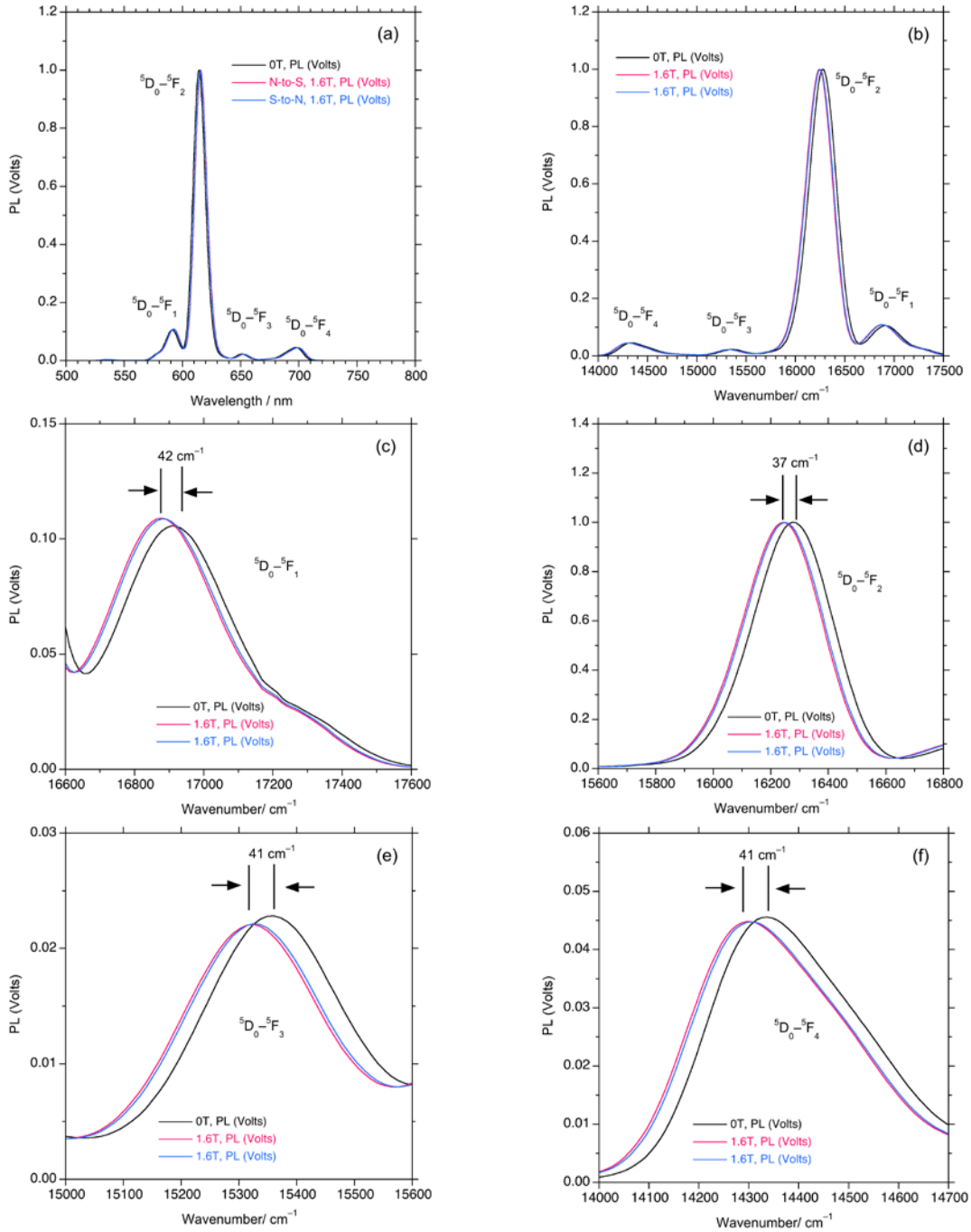

Fig. S7. Comparison of normalized PL spectra of $Eu^{III}(hfa)_3$ in $CHCl_3$ solution. 1.0×10^{-3} M: λ_{ex} = 300 nm. Pathlength = 5 mm in the absence of 1.6 T (black line) and in the presence of 1.6 T with N-up (red line) and with S-up (blue line) configurations as functions of (a) wavelength in nm and (b–f) of wavenumber in cm^{-1}.

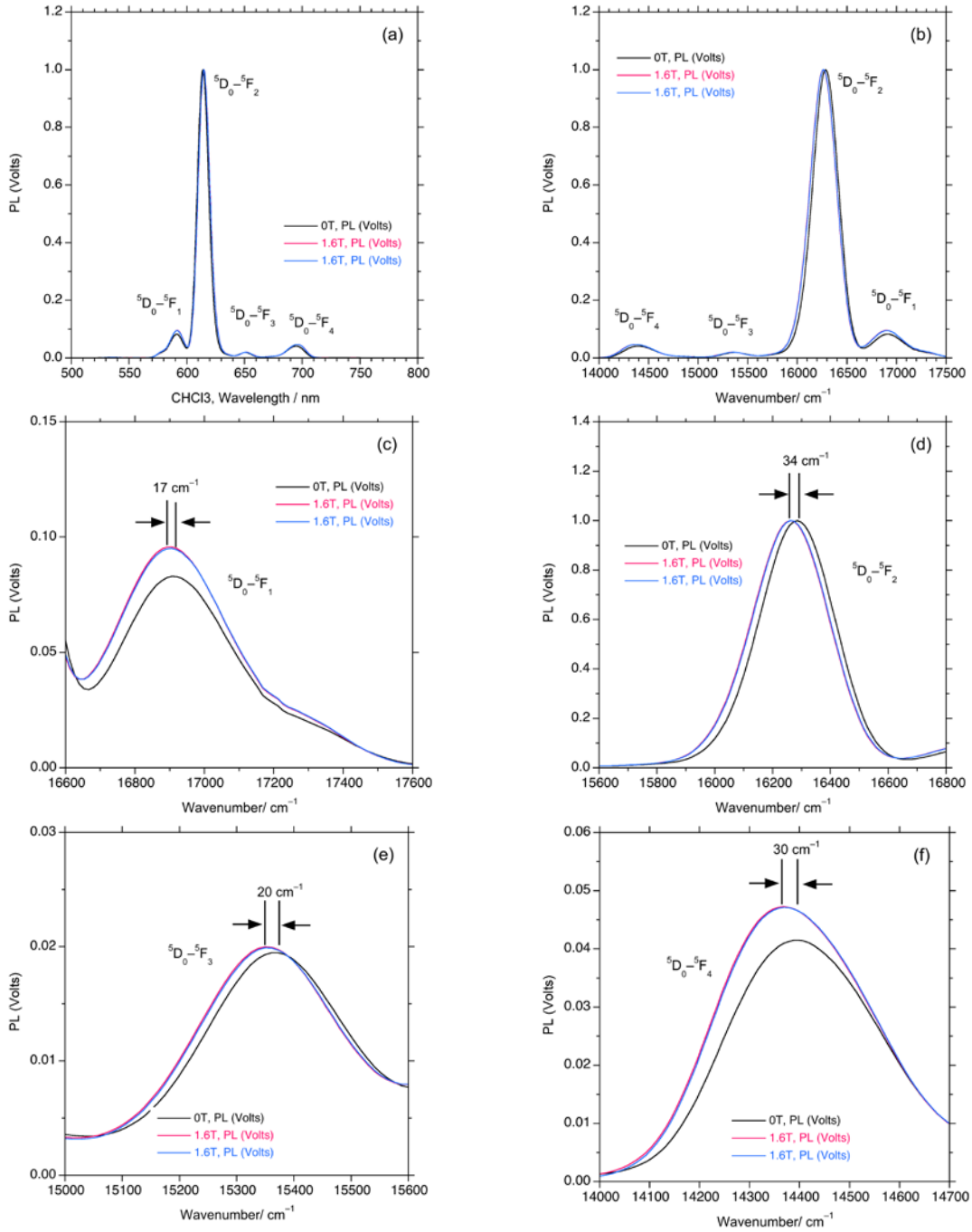

Fig. S8. Comparison of normalized PL spectra of $Eu^{III}(hfa)_3$ in acetone solution. 1.0×10^{-3} M: λ_{ex} = 330 nm. Pathlength = 5 mm in the absence of 1.6 T (black line) and in the presence of 1.6 T with N-up (red line) and with S-up (blue line) configurations as functions of (a) wavelength in nm and (b–f) of wavenumber in cm^{-1}.

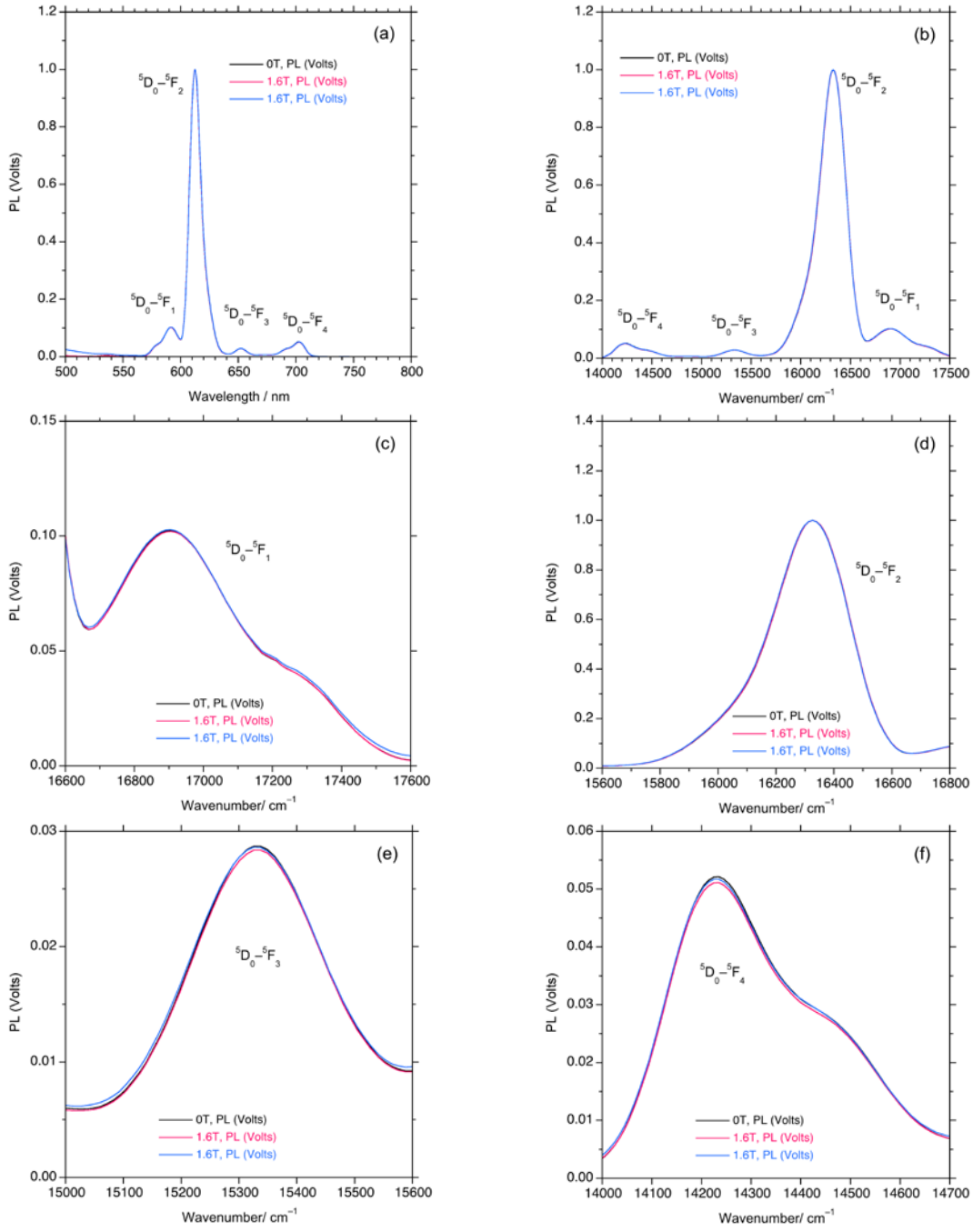

Fig. S9. Comparison of normalized PL spectra of $Eu^{III}(acac)_3$•Phen in $CHCl_3$ solution. 1.0×10^{-3} M: λ_{ex} = 300 nm. Pathlength = 5 mm in the absence of 1.6 T (black line) and in the presence of 1.6 T with N-up (red line) and with S-up (blue line) configurations as functions of (a) wavelength in nm and (b–f) of wavenumber in cm^{-1}.

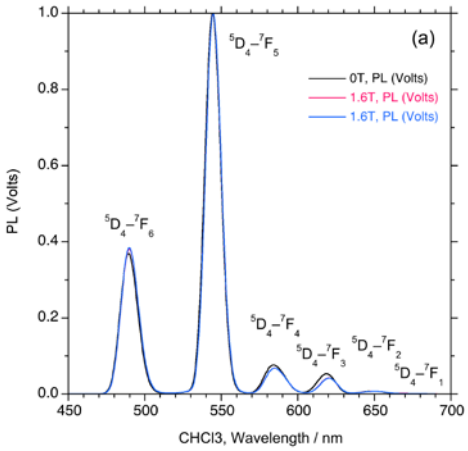
(a)
0T, PL (Volts)
1.6T, PL (Volts)
1.6T, PL (Volts)
$^5D_4$–$^7F_5$
$^5D_4$–$^7F_6$
$^5D_4$–$^7F_4$
$^5D_4$–$^7F_3$
$^5D_4$–$^7F_2$
$^5D_4$–$^7F_1$
PL (Volts)
CHCl3, Wavelength / nm

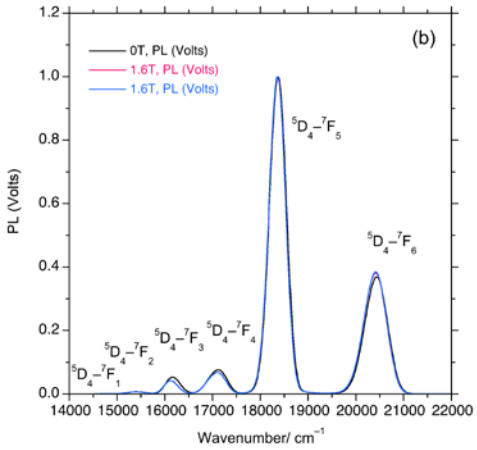
(b)
0T, PL (Volts)
1.6T, PL (Volts)
1.6T, PL (Volts)
$^5D_4$–$^7F_5$
$^5D_4$–$^7F_6$
$^5D_4$–$^7F_4$
$^5D_4$–$^7F_3$
$^5D_4$–$^7F_2$
$^5D_4$–$^7F_1$
PL (Volts)
Wavenumber/ cm^{-1}

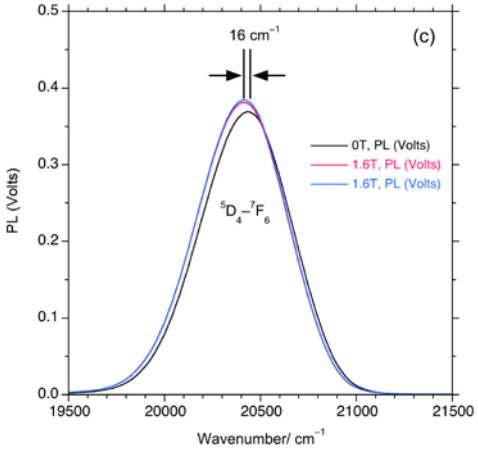
(c)
16 cm^{-1}
0T, PL (Volts)
1.6T, PL (Volts)
1.6T, PL (Volts)
$^5D_4$–$^7F_6$
PL (Volts)
Wavenumber/ cm^{-1}

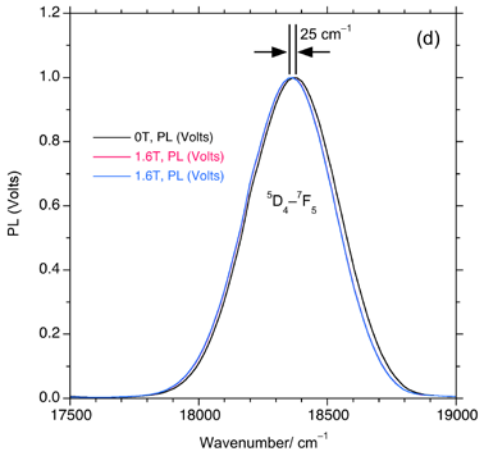
(d)
25 cm^{-1}
0T, PL (Volts)
1.6T, PL (Volts)
1.6T, PL (Volts)
$^5D_4$–$^7F_5$
PL (Volts)
Wavenumber/ cm^{-1}

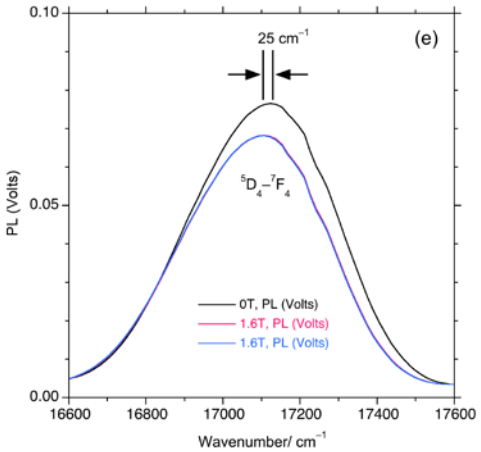
(e)
25 cm^{-1}
$^5D_4$–$^7F_4$
0T, PL (Volts)
1.6T, PL (Volts)
1.6T, PL (Volts)
PL (Volts)
Wavenumber/ cm^{-1}

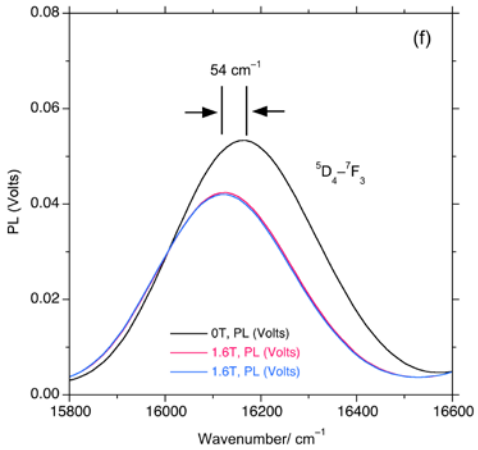
(f)
54 cm^{-1}
$^5D_4$–$^7F_3$
0T, PL (Volts)
1.6T, PL (Volts)
1.6T, PL (Volts)
PL (Volts)
Wavenumber/ cm^{-1}

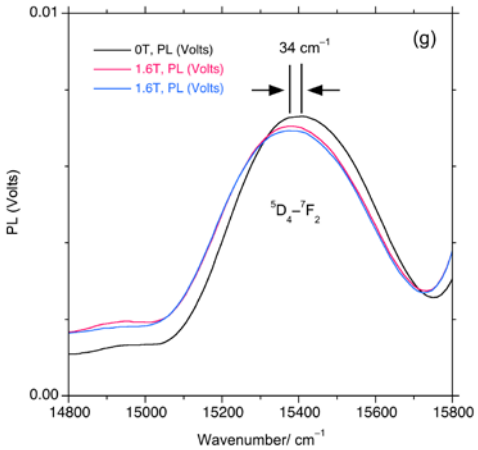
(g)
0T, PL (Volts)
1.6T, PL (Volts)
1.6T, PL (Volts)
34 cm^{-1}
$^5D_4$–$^7F_2$
PL (Volts)
Wavenumber/ cm^{-1}

Fig. S10. Comparison of normalized PL spectra of $Tb^{III}(hfa)_3$ in $CHCl_3$ solution. 1.0×10^{-3} M: λ_{ex} = 300 nm. Pathlength = 5 mm in the absence of 1.6 T (black line) and in the presence of 1.6 T with N-up (red line) and with S-up (blue line) configurations as functions of (a) wavelength in nm and (b–g) of wavenumber in cm^{-1}.

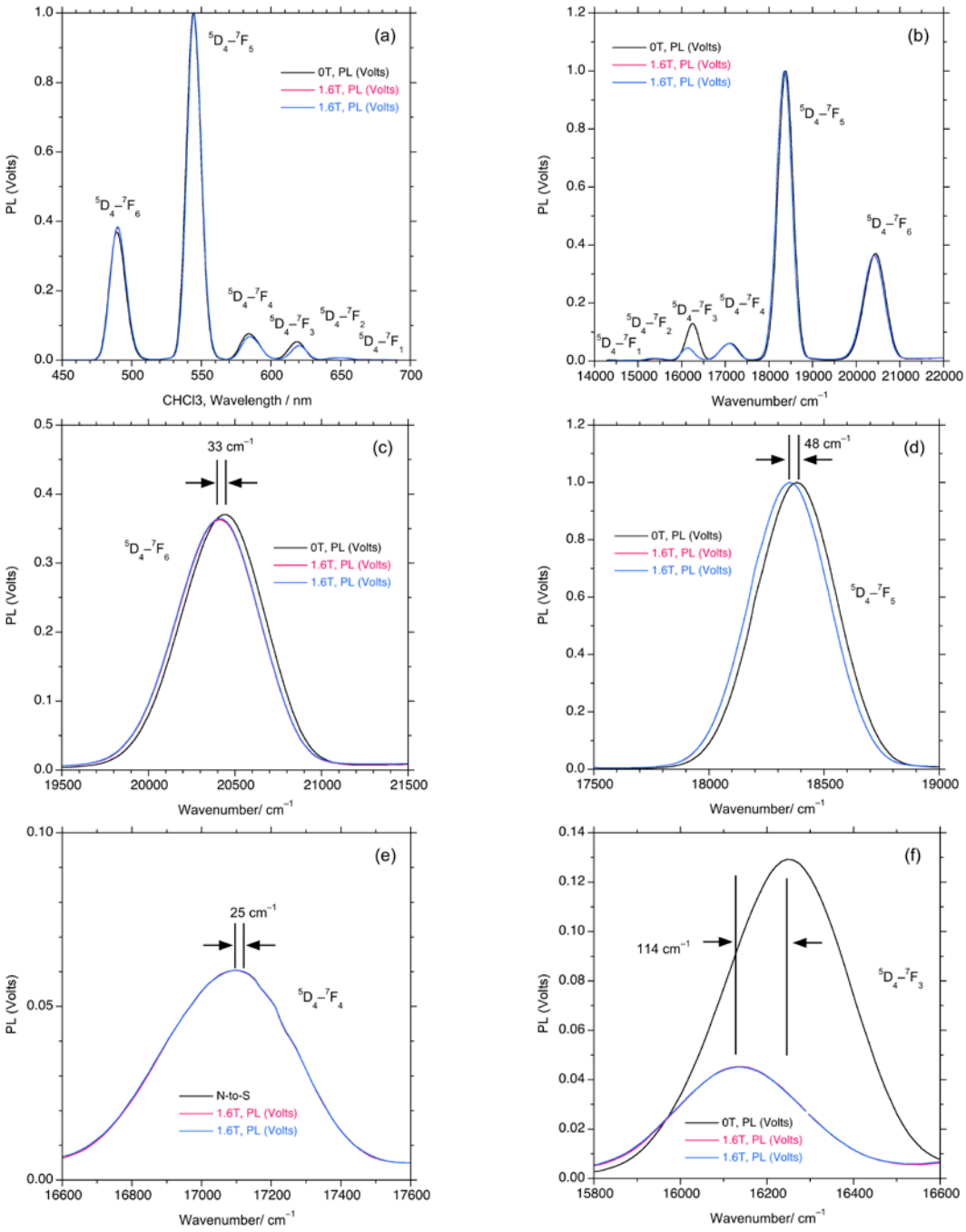

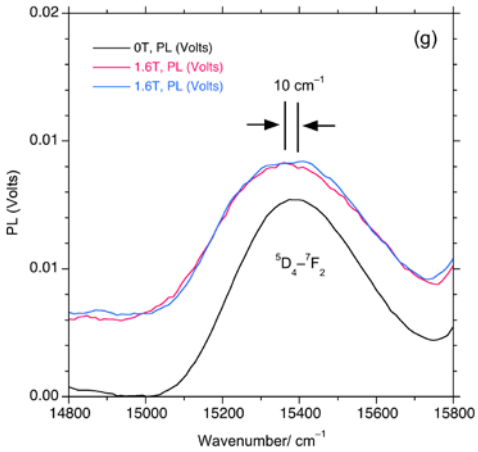

Fig. S11. Comparison of normalized PL spectra of $Tb^{III}(hfa)_3$ in acetone solution. 1.0×10^{-3} M: λ_{ex} = 330 nm. Pathlength = 5 mm in the absence of 1.6 T (black line) and in the presence of 1.6 T with N-up (red line) and with S-up (blue line) configurations as functions of (a) wavelength in nm and (b–g) of wavenumber in cm^{-1}.

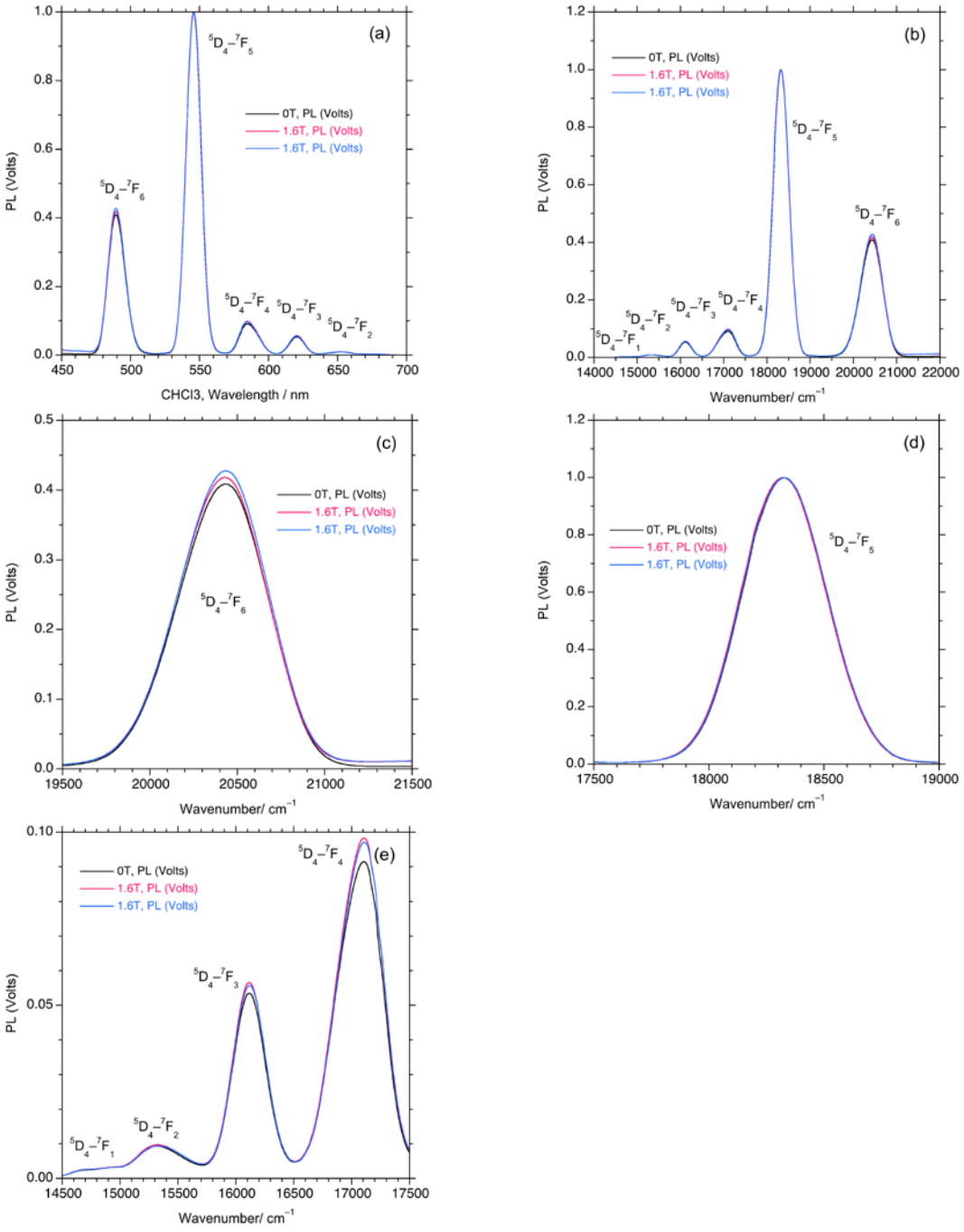

Fig. S12. Comparison of normalized PL spectra of $Tb^{III}(acac)_3$•Phen in $CHCl_3$ solution. 1.0×10^{-3} M: λ_{ex} = 300 nm. Pathlength = 5 mm in the absence of 1.6 T (black line) and in the presence of 1.6 T with N-up (red line) and with S-up (blue line) configurations as functions of (a) wavelength in nm and (b–e) of wavenumber in cm^{-1}.